Article

Analysis of Particle Emissions from a Jet Engine Including Conditions of Afterburner Use

Remigiusz Jasiński

Faculty of Civil and Transport Engineering, Poznan University of Technology, 60-965 Poznan, Poland; remigiusz.jasinski@put.poznan.pl

Abstract: Particle emissions from aircraft engines are mainly related to the emission of particles with very small diameters. The phenomena of the formation of particles in various operating conditions of turbine engines are known. However, it is difficult to find the results of research on the use of the afterburner in the literature. Increased aviation activity within military airports and situations such as air shows are associated with a very intense emission of particles, and pose a direct threat to human health. This article presents an analysis of particulate matter emissions from a military aircraft engine, with particular emphasis on operation with an afterburner. The parameters of the emission of particles determined were: PM Number Emissions Index (EI_N), Particle Number Emissions Intensity (E_N), PM Mass Emission Index (EI_M), PM Mass Emission Intensity (E_M), Differential Particle Number Emission Index, Differential Particle Volume Emission Index, and Differential Particle Mass Emission Index. The value of EI_N for the afterburner use was the lowest among the whole operation range of the engine and was equal to 1.3×10^{15} particles per kilogram. The use of an afterburner resulted in a sharp increase in the EI_M coefficient, which reached 670 mg/kg. Despite a very large increase in fuel consumption, the EI_M coefficient turned out to be over 60 times greater than in the case of 100% engine thrust.

Keywords: jet engine; afterburner; emission; particles; particulate matter

1. Introduction

Global policy and research place great emphasis on reducing greenhouse gas emissions from various modes of transport, including air transport [1–3]. Undoubtedly, climate action is one of humanity's key activities. However, it should be remembered that the quality of the air we breathe is a separate issue. Research shows that air pollution in urban agglomerations is high, to which transport clearly contributes [4–6]. Apart from road transport, air transport is very important regarding the emission of toxic compounds [7]. This is due to the emission of a large number of fine particles, which is especially dangerous for the human body [8,9].

The results of scientific research [10,11] confirm that the emission of particles from aircraft engines has a negative impact on air quality on a local scale. In the coming years, the impact of aviation on air in areas adjacent to airports will increase due to the forecasted development of the aviation sector and increasing transport volume. Despite the aviation crisis related to the COVID-19 pandemic, aviation is likely to return to dynamic development [12].

The effects of air pollution with exhaust emission compounds include premature mortality as well as cardiovascular and respiratory diseases. In addition, the strong carcinogenic effect of hydrocarbon compounds and particulate matter is shown in diseases, particularly in the elderly and children [13–15]. In the case of aviation and its impact on air quality, the local aspect is crucial. The risk is mainly borne by residents in the vicinity of airports and ground service [16]. Test results indicate that the area of the airport may be contaminated with particles at the level of a very heavily loaded road communication

junction. These situations put people at risk of becoming ill due to long-term exposure to pollution [17]. It is also important to remember the effects of short-term exposure of the body to pollution. Reference [18] indicates detrimental heart effects from short-term exposure to PM2.5. One example of short-term but intense exposure to air pollution is air shows in which military planes take part, which are characterized by extremely high fuel consumption and exhaust emissions. In addition, the shows are performed on a small ceiling, in close proximity to the audience. It remains an open question to what extent pollutant emissions can suddenly affect air quality. Research shows that single landing operations of aircraft can significantly increase the concentration of particles in the area adjacent to the airport [11].

Commonly used methods to reduce the impact of aviation on the environment are the use of biofuels, appropriate airspace management and technical solutions (e.g., introducing alternative drives), and biofuels used as a blend with fossil fuels to help reduce greenhouse gas emissions. Additionally, biofuels have a positive effect on exhaust emissions [19–22]. The inevitable electrification of aviation is a difficult process due to the insufficiently high energy density of the batteries used. There are an increasing number of solutions for electric sprouts that use hydrogen as a fuel for fuel cells, but these are solutions that are not used on a large scale [23,24].

What is new is the introduction of the regulation for the certification of aircraft engines in the field of particulate matter emissions. Scientific publications [25,26] indicate that airport operations (taxiing, take-off, and landing) below 950 m, included in the LTO test (Landing and Take-off Cycle), have a major impact on air quality in the local aspect. Due to the LTO test disadvantages resulting from the limitation to smoke number measurements (exhaust transparency), tests are carried out to improve the approval process and extend it by measuring the number and mass of particles. This solution will allow the gathering of data on particle emissions from newly manufactured engines, and will create the opportunity to improve models for estimating pollutant emissions from transport sources according to CAEP/10 nvPM certification requirements [27].

In the case of military aircraft, emissions are of secondary importance. The priority is that the fighter or military transport aircraft is designed to perform missions with specific objectives. In addition, military aviation has a very small share of the total air traffic. Therefore, it is minimally responsible for air pollution and climate change. However, it is worth considering the short-term emissions experienced by people at air shows or by personnel at military bases during ground handling. In particular, the operation of an engine with the use of an afterburner is likely associated with an incomparably greater emission of particulate matter than in the case of normal values of engine parameters.

The subject of particulate matter emissions from military aircraft engines has been discussed in many publications [28–32]. The main topic of this publication is the parameterization of particles in the entire engine load range. Few publications deal with the use of an afterburner [33,34], especially with the emission issue. The aim of the research presented in the article was to evaluate the emission of particles from a military fighter using an afterburner.

2. Materials and Methods

2.1. Test Engine, Fuels, Operating Schedule

The tested engine was a Pratt & Whitney F100-PW-229. It is an engine with a low bypass ratio and is the propulsion engine of the F-16 fighter. Basic technical data are presented in Table 1.

The engine was powered by JP-8 fuel (F-34 military jet kerosene). It is light distillate fuel that consists of a mixture of complex hydrocarbons, such as 50–65% paraffins, 10–20% aromatics, and 20–30% naphthenes [35]. JP-8 fuel is similar to the Jet A-1 aviation kerosene commonly used in civil aviation. The main difference between these fuels is the presence of anti-corrosion and anti-icing additives in JP-8.

Table 1. Technical specification of the F100-PW-229 engine.

Maximum thrust	73.13 kN
Maximum thrust with afterburner	128.91 kN
Specific Fuel Consumption (for maximum thrust)	0.693 kg/kN·h
Specific Fuel Consumption with afterburner	2.6 kg/kN·h
Bypass ratio	0.36
Weight	1370 kg

The F100-PW-229 engine was tested regarding particle emissions, with particular emphasis on afterburner use. The tests were carried out at the 31st Tactical Aviation Base in Krzesiny. During the tests, military infrastructure was used, including a test bench for testing engines after performed services. The test bench enabled the measurement of thermodynamic parameters (temperature and pressure at various points of the engine) and fuel consumption. The tests were carried out during one day, and the ambient conditions were temperature in the range of 12–17 °C and an atmospheric pressure of 1000.1 hPa.

Table 2 presents the scope of the engine tests performed, taking into account the average sample temperature and fuel flow. The aim of the first test was to assess the correctness of the apparatus indications and to technically assess the engine operation. The results of the measurements from the first sample were not taken into account in the analysis of the test results. The main tests of the engine were tests 2, 3, and 4. In all tests, the concentration of particles was measured at 10 points of the engine operation, which in the table are indicated by the fuel flow rate. The measurement at each point of the engine operation lasted approximately 180 s. The fuel flow values for engine operation with the use of the afterburner are underlined. The power lever controlled the engine operation. The position of the power lever is presented in further analyses as the relative position of the power lever (Z%). Because, in individual tests, the relative position of the power lever differed slightly, the results from all tests were averaged, and the emission of particles was presented in relation to the power lever position ranges.

Table 2. Engine test matrix.

Test Number	Fuel Type	Average Sample Gas Temperature (°C)	Fuel Flow Rate (kg/h)
1-pretest, warm	JP-8	15.4 ± 0.1	512; 1200; 2570; 25,878 ±3%
2	JP-8	15.9 ± 0.1	512; 801; 1190; 1305; 1743; 2388; 2568; 4419; 5835; 25,878 ± 3%
3	JP-8	16.1 ± 0.1	510; 799; 1210; 1306; 1744; 2382; 2570; 4420; 5830; 25,878 ± 3%
4	JP-8	15.8 ± 0.1	512; 802; 1191; 1307; 1749; 2381; 2561; 4413; 5843; 25,878 ± 3%

2.2. Apparatus and Procedures

A portable apparatus was used to measure the particle size distribution (PSD), the concentration of carbon dioxide, and the temperature of the sample. The measurement path was 3 m long, taking into account that the measuring probe was made of stainless steel, which is non-reactive at high temperatures. In accordance with ICAO recommendations, a cyclone was used to remove particles of very large dimensions, preventing calculation errors and keeping the measuring device clean. The main probe was placed 25 m from the engine outlet, as indicated in the literature [36,37]. Taking measurements at a distance from the engine allows for measurements in the entire range of its operation, which is particularly important when an afterburner is used. In addition, it allows most of the chemical reactions and particle formation processes to complete [28].

A TSI 3090 EEPS (Engine Exhaust Particle Sizer) was used to measure the particle size distribution. This device measures the concentration of particles in the size range of 5.6 nm to 560 nm. The measurements were performed with a frequency of 1 Hz. During the research, a Semtech DS analyzer was used, the main purpose of which was to measure the concentration of carbon dioxide.

2.3. Data Analyses

Data collected by the TSI 3090 EEPS ensured the concentration of particles and particle size distribution from the tested engine throughout the whole range of engine operation, including afterburner use. The differential number particle size distribution, dCN/d logDp, at a specified fuel flow rate (relative position of the power lever) was obtained by averaging the particle numbers recorded under the same engine operating condition from the same instrument particle size bins. The results obtained during the three tests were averaged and assigned to the appropriate ranges of the relative position of the power lever.

The indicators for the particulate mass were determined on the basis of the results of particle size distributions, taking into account the appropriate density of particles depending on their diameter [38]. On this basis, three groups of particle indicators have been indicated:

- Particle Number Emission Indices: PM Number Emissions Index (EI_N) and Particle Number Emissions Intensity (E_N);
- PM Mass Emission Indices: PM Mass Emission Index (EI_M) and PM Mass Emission Intensity (EI_M);
- Particle size distribution: Differential Particle Number Emission Index, Differential Particle Volume Emission Index, Differential Particle Mass Emission Index.

3. Results

3.1. Particle Number Emission Indices

Figure 1 shows average PM Number Emission Indices (EI_Ns) and their associated error calculated from the EEPS data for the different relative positions of the power lever. Overall, there was a clear downtrend in the value of EI_N with increasing engine thrust. The average EI_N decreased from 1.1×10^{16} to 5.8×10^{15} particles per kilogram as the engine relative position of the power lever increased from 30% to 100%. Along with the power lever's position increase from 14% to 30%, a slight increase in the EI_N was observed. Figure 1 also shows that afterburner use resulted in a significant decrease in PM Number Emission Indices compared to the typical operating range of the engine. The value of EI_N for the afterburner use was the lowest among the rest of the operation range of the engine. This phenomenon was related to the drastic increase in fuel flow during the use of the afterburner, which was approximately 20,000 kg/h compared to the maximum position of the power lever (100%).

Particle Number Emissions Intensity (E_N) is also shown in Figure 1. An increase of E_N in the entire tested range of engine operation was found. This increase occurred because increasing the thrust increased fuel consumption, hence leading to the formation of more particles over time. The lowest E_N value was found in the range of the power lever position of <14; 20)%, equal to 1.8×10^{15} particles/s, and the highest for afterburner use (9.8×10^{16} particles/s). It is worth noting that using the afterburner compared to the maximum position of the power lever resulted in an increase in E_N by only 10%.
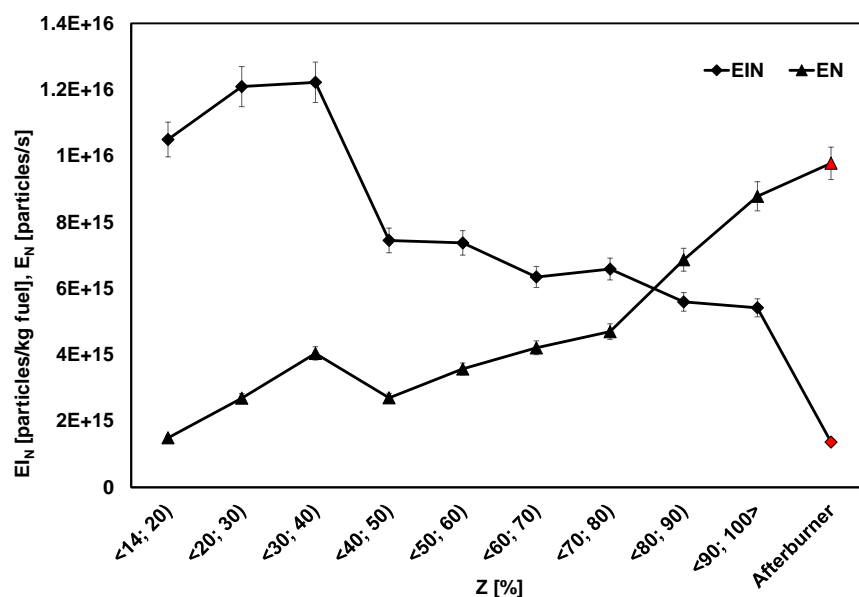
Figure 1. Particle Number Emissions Index (EI_N) and Particle Number Emissions Intensity (E_N) versus relative position of the power lever (Z).

3.2. PM Mass Emission Indices

The PM Mass Emission Indices (EI_Ms) under various engine thrust values (power lever positions) were calculated from the EEPS measurements. Figure 2 shows how EI_M changed while increasing the engine thrust. For low thrust values, the highest EI_M values were found in the standard engine operation. The EI_M value was a maximum of 33 mg/kg for engine operation in the range of the power lever position <30; 40)%. In the case of engine operation with medium and high thrust values, a significant decrease in the EI_M coefficient was found, which fluctuated in the range of 8–16 mg/kg. The use of the afterburner resulted in a sharp increase in the EI_M coefficient (it reached 670 mg/kg). Despite a very large increase in fuel consumption, the EI_M coefficient was over 60 times greater than in the case of 100% thrust. This increase proves the formation of very large particles that are of key importance in terms of mass emission.
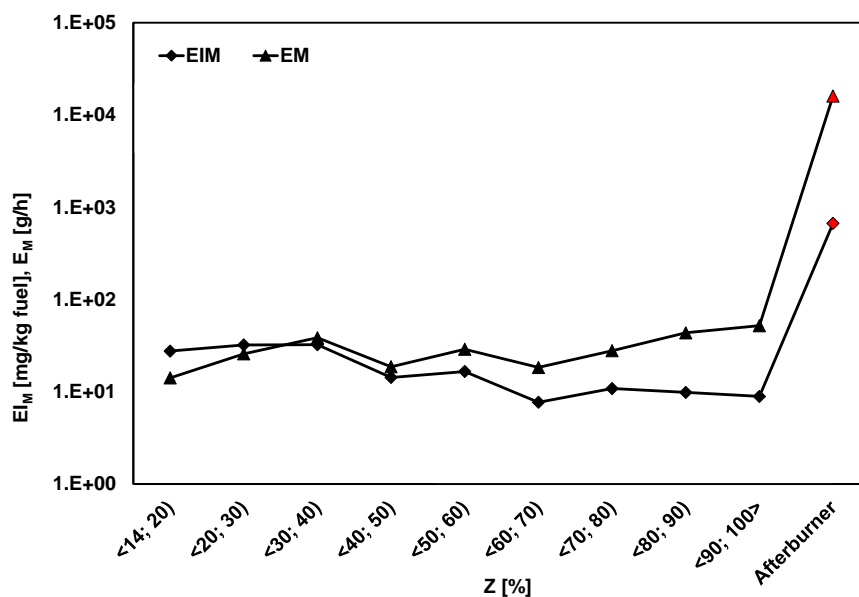

Figure 2. PM Mass Emission Index (EI_M) and PM Mass Emission Intensity (E_M) versus relative position of the power lever (Z).

PM mass emission intensity (E_M) is also shown in Figure 2. It is difficult to indicate a clear relationship between E_M and thrust. In the power lever position range of <14; 70)%, fluctuations in the E_M value in the range of 14–38 g/h can be noticed in the figure. It can be clearly observed that in the case of large values of the power lever position <60; 100>% mass emitted increased to a maximum value of 53 g/h. The use of the afterburner was associated with an entirely different nature of particulate matter emissions. The E_M indicator during afterburner use was equal to 16,000 g/h. Such a high mass emission of particulate matter indicates completely different processes of particle formation during the use of the afterburner.

3.3. Particle Size Distribution

The data recorded by the EEPS was averaged in the defined power lever position ranges and then converted to differential number-based ($dEI_N / d\ logD_p$), differential volume-based ($dEI_V / d\ logD_p$), and differential mass-based ($dEI_M / d\ logD_p$) particle size distributions.

Figure 3 represents plots of $dEI_N / d\ logD_p$ under different thrust values (represented by power level position). The particles formed in the nucleation mechanism (diameter 5–50 nm) dominated PN emission, which is characteristic of jet engines. Thus, number-based PSDs exhibited a single-mode log-normal distribution for the whole range of engine operation except afterburner use. PSDs based on the number of particles indicated that particles with diameters greater than 100 nm were practically non-existent. The center of the nucleation mode peaks showed some changes with thrust for the number PSDs. Their magnitude decreased as thrust increased.
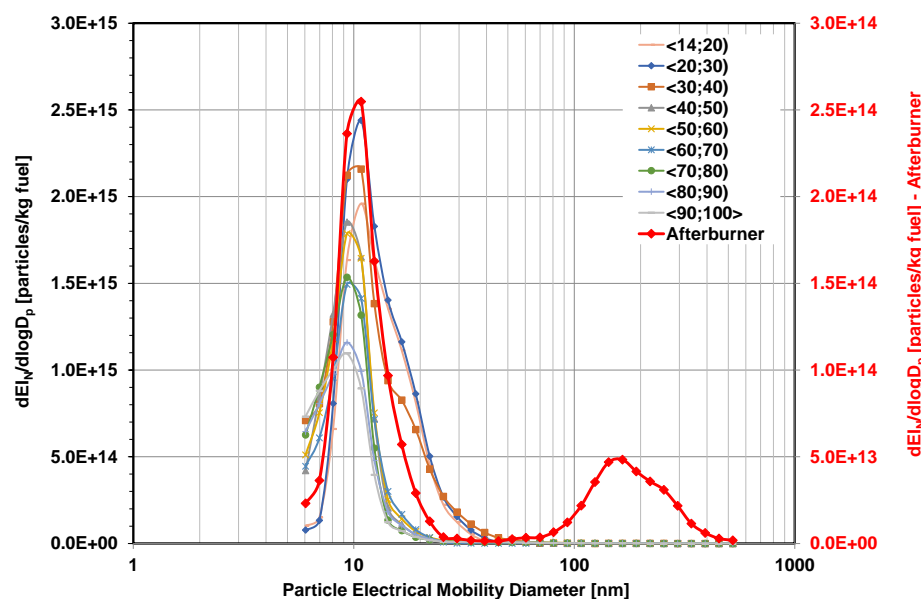

Figure 3. Differential Particle Number Emission Index (EI_N) PSD for the entire range of engine operation and the afterburner.

The particle size distribution of EI_N under the condition of afterburner use is clearly bimodal. In addition to the clear nucleation mode, there was a noticeable soot mode associated with the formation of a large number of particles with diameters greater than 100 nm (Figure 3—auxiliary axis). The value in the nucleation mode peak was the lowest among all the engine operating conditions (2.55×10^{14} particles/kg), as it was associated with very high fuel consumption. The maximum value of the soot mode was 5×10^{13} particles/kg. The presented PSD clearly differs from the single-mode PSD characteristic for the operation of a jet engine.

Figure 4 shows the Differential Particle Volume Emission Index (EI$_V$) PSD. A characteristic bimodal dimensional distribution can be observed in each tested case (excluding the afterburner). A certain number of particles with diameters greater than 30 nm and 100 nm were formed, providing a bimodal PSD. The center of the nucleation mode peaks changed with increasing thrust. It is clearly visible that for the range of the power lever position <14; 40)%, the center of the nucleation mode peaks were for a diameter value of 20 nm. For the other values of the power lever position, the center was at a diameter of 10 nm. Increasing the thrust resulted in the formation of particles in a soot mode due to the coagulation and condensation of sulfur and aromatic hydrocarbons. The center of the soot mode peaks and values did not noticeably change with increasing thrust.
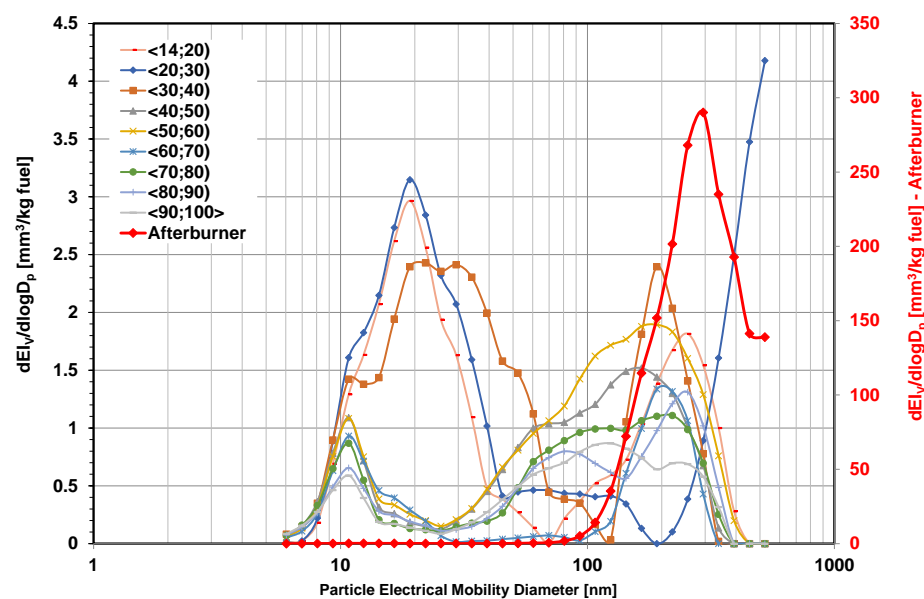

Figure 4. Differential Particle Volume Emission Index (EI$_V$) PSD for the entire range of engine operation and the afterburner.

Unlike all other particle size distributions, particle characteristics during afterburner use were unimodal (Figure 4—auxiliary axis). The nucleation mode was imperceptible due to the absolute dominance of the soot mode. The center of the soot mode peak was for a diameter value of 300 nm. The maximum value of this EI$_V$ was equal to 275 mm^3/kg, which is approximately 300 times greater than when the engine was operated with maximum thrust.

Figure 5 shows the Differential Particle Mass Emission Index (EI$_M$) PSD. It was found that the particle size distributions in the case of EI$_M$ were bimodal, with the exception of the use of the afterburner. In nucleation mode, particles with diameters 10–20 nm dominated, with a tendency to shift the distribution towards a smaller diameter with increasing thrust. The maximum EI$_M$ value was found for the power lever position <20; 30)%, equal to 3.8 mg/kg. The centers of the soot mode peaks were around particles with diameters of 200 nm, and peak values did not change substantially with increasing thrust.

The particle size distribution obtained during afterburner use was unimodal (Figure 5—auxiliary axis). The dominant mode was the soot mode, with a maximum value of 95 mg/kg corresponding to a particle with a diameter of about 300 nm.
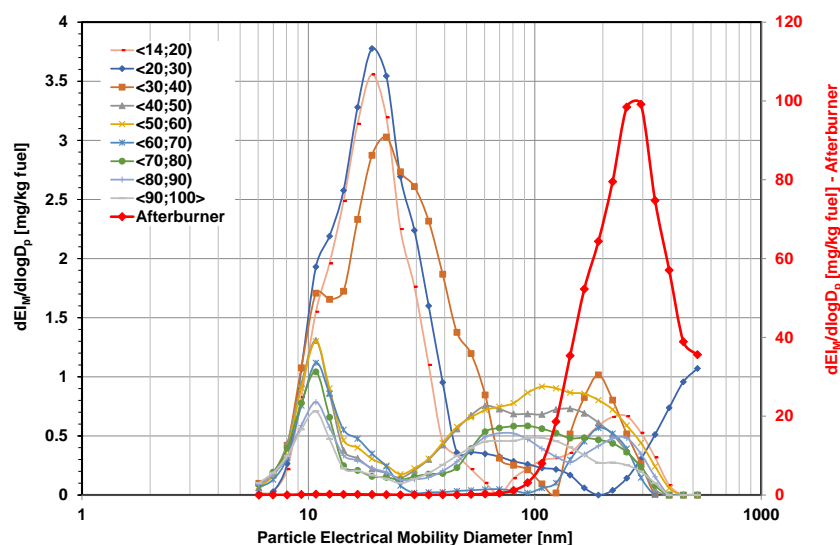
Figure 5. Differential Particle Mass Emission Index (EI$_M$) PSD for the entire range of engine operation and the afterburner.

4. Discussion

The determined Particle Number Emissions Index (EI$_N$) shows the dependence on the thrust. References [39–41] indicate that, in many cases, the EI$_N$ vs. thrust relationship results in U-shaped curves. However, Reference [40] shows the example of the CFM56-5B4/2P engine, in which the U-shape was not shown. Furthermore, it is highly similar to the one obtained in our research. Research also shows that the EI$_N$ coefficient does not always have the highest values for the maximum thrust. Reference [42] indicates a lower EI$_N$ coefficient during take-off than is the case of many turbofan engines. Moreover, [43] indicates that the EI$_N$ decreases along with the fuel flow over the entire engine operational range. In the case of research on a military engine, a low bypass ratio should be taken into account. A significant part of the thrust generated in high-bypass engines results from the air flowing through the engine, and in the case of a military engine, the thrust generated by fuel combustion dominates, which has a significant impact on the EI$_N$ values depending on the thrust force.

Most research sources [40,41] point to the EI$_M$ vs. thrust indicator as a U-shape curve. The results of this research showed that the EI$_M$ index decreased with increasing fuel flow. However, contrary to most of the literature, there was no increase in EI$_M$ for very high thrust values. This lack of increase is due to the small soot mode seen on the PSD (Figure 5). A very large increase in EI$_M$ can be noticed for the use of the afterburner, where the soot mode absolutely dominated.

The obtained particle size distributions are confirmed in the literature [41,42]. Lognormal EI$_N$ PSD is a classic image for a jet engine. In the case of EI$_M$ PSD, bimodal distributions were obtained, which is also characteristic, but with the maximum value in the nucleation mode, not soot mode. This is confirmed in the literature [42], and the obtained distribution is the closest to that obtained for the General Electric CF6 engine. The indicators obtained for the use of the afterburner are difficult to reference in the literature. However, the knowledge of the engine processes accompanying engine operation with the afterburner allows for the substantiation of the obtained results.

The literature makes clear that airport operations significantly affect air pollution with particles [44]. An engine's operation in landing conditions at a height of approximately 50 m caused a several-dozen-times increase in the concentration of nanoparticles in the air near the ground. The presented research results indicate that afterburner use changes particulate matter emission on a completely different scale. Therefore, it seems interesting to continue research in the field of air quality in the areas adjacent to the airports with increased military flights. The aspect of air quality during events such as air shows is also

interesting from the perspective of the high intensity of jet aircraft flights, whose engines often work in very dynamic conditions, also using an afterburner.

One of the main conclusions based on the research carried out is that a large number of particles with diameters greater than 200 nm are formed during the use of an afterburner. Measurement devices intended for the study of particulate emissions from internal combustion engines often limit the measurement range of the particle diameters to about 550 nm. This limitation is due to the assumption that internal combustion engines (particularly jet engines) do not generate particles with larger diameters. The presented data show a probability that a jet engine operating with an afterburner generates particles larger than 500 nm, which may affect the emission factors related to the mass of particulate matter.

5. Conclusions

Research was carried out on the emission of particulate matter from a jet engine, the main purpose of which was to determine the particle emission indexes for engine operation with an afterburner. A comparative analysis of the particulate matter emission coefficients for various engine operating conditions was performed, and the obtained PSDs were analyzed.

The analysis shows that increasing the engine thrust reduced PM Number Emission Indices (EI_Ns), especially in the case of using an afterburner. Particulate Matter Emission Intensity (E_N) increased with the increasing thrust of the jet engine, reaching the maximum value when the afterburner was used.

PM Mass Emission Indices decreased with increasing thrust, but the use of an afterburner resulted in a sharp increase in PM Mass Emission Index (EI_M) and PM Mass Emission Intensity (E_M) due to the high emission of particles with diameters greater than 200 nm.

The obtained PSDs indicate a clear bimodality in the case of engine operation with an afterburner. Large values of the soot mode for working with the afterburner are of key importance for the PM Mass Emission Indexes.

Further work directions include the assessment of the impact of afterburner use on air quality during take-off operations and maneuvers during events such as air shows, where people are exposed to high concentrations of nanoparticles in the air.

References

1. Epstein, A.H.; O'Flarity, S.M. Considerations for Reducing Aviation's CO_2 with Aircraft Electric Propulsion. *J. Propuls. Power* **2019**, *35*, 572–582. [CrossRef]
2. Carlsson, F.; Hammar, H. Incentive-based regulation of CO_2 emissions from international aviation. *J. Air Transp. Manag.* **2002**, *8*, 365–372. [CrossRef]
3. Hassan, M.; Pfaender, H.; Mavris, D. Probabilistic assessment of aviation CO_2 emission targets. *Transp. Res. Part D Transp. Environ.* **2018**, *63*, 362–376. [CrossRef]
4. Jasiński, R.; Galant-Gołębiewska, M.; Nowak, M.; Ginter, M.; Kurzawska, P.; Kurtyka, K.; Maciejewska, M. Case Study of Pollution with Particulate Matter in Selected Locations of Polish Cities. *Energies* **2021**, *14*, 2529. [CrossRef]
5. Han, L.; Zhou, W.; Pickett, S.T.; Li, W.; Qian, Y. Multicontaminant air pollution in Chinese cities. *Bull. World Health Organ.* **2018**, *96*, 233–242E. [CrossRef] [PubMed]
6. Nowak, M.; Andrzejewski, M.; Galant-Gołębiewska, M.; Rymaniak, L. Simulation assessment of the selected combination of road and rail infrastructure in the aspect of choosing the route of road transport means. *AIP Conf. Proc.* **2019**, *2078*, 020055. [CrossRef]
7. Karpiuk, W.; Borowczyk, T.; Idzior, M.; Smolec, R. The Evaluation of the Impact of Design and Operating Parameters of Common Rail System Fueled by Bio-Fuels on the Emission of Harmful Compounds. *DEStech Trans. Environ. Energy Earth Sci.* **2016**, 16–22. [CrossRef]

8. Atkinson, R.W.; Mills, I.C.; Walton, H.; Anderson, H.R. Fine particle components and health—A systematic review and meta-analysis of epidemiological time series studies of daily mortality and hospital admissions. *J. Expo. Sci. Environ. Epidemiol.* **2014**, *25*, 208–214. [CrossRef]
9. Englert, N. Fine particles and human health—A review of epidemiological studies. *Toxicol. Lett.* **2004**, *149*, 235–242. [CrossRef]
10. Przespolewska-Gdowik, K.; Jasiński, R. Analysis of the Nicolaus Copernicus Airport Activity in Terms of the Flight Operations Impact on Air Pollution. *Energies* **2021**, *14*, 8236. [CrossRef]
11. Jasinski, R. Mass and number analysis of particles emitted during aircraft landing. *E3S Web Conf.* **2018**, *44*, 00057. [CrossRef]
12. Dube, K.; Nhamo, G.; Chikodzi, D. COVID-19 pandemic and prospects for recovery of the global aviation industry. *J. Air Transp. Manag.* **2021**, *92*, 102022. [CrossRef]
13. Fantke, P.; Jolliet, O.; Evans, J.S.; Apte, J.; Cohen, A.J.; Hänninen, O.; Hurley, F.; Jantunen, M.J.; Jerrett, M.; Levy, J.I.; et al. Health effects of fine particulate matter in life cycle impact assessment: Findings from the Basel Guidance Workshop. *Int. J. Life Cycle Assess.* **2014**, *20*, 276–288. [CrossRef]
14. Chiarini, B.; D'Agostino, A.; Marzano, E.; Regoli, A. Air quality in urban areas: Comparing objective and subjective indicators in European countries. *Ecol. Indic.* **2020**, *121*, 107144. [CrossRef]
15. Koolen, C.D.; Rothenberg, G. Air Pollution in Europe. *ChemSusChem* **2019**, *12*, 164–172. [CrossRef] [PubMed]
16. Jasiński, R. Number and mass analysis of particles emitted by aircraft engine. *MATEC Web Conf.* **2017**, *118*, 00023. [CrossRef]
17. Chen, J.; Hoek, G. Long-term exposure to PM and all-cause and cause-specific mortality: A systematic review and meta-analysis. *Environ. Int.* **2020**, *143*, 105974. [CrossRef]
18. Bae, H.J. Effects of short-term exposure to PM10 and PM2.5 on mortality in Seoul. *Korean J. Environ. Health Sci.* **2021**, *40*, 346–354. [CrossRef]
19. Karpiuk, W.; Smolec, R.; Idzior, M. DME Use in Self-Ignition Engines Equipped with Common Rail Injection Systems. *DEStech Trans. Environ. Energy Earth Sci.* **2016**, 37–43. [CrossRef]
20. Przysowa, R.; Gawron, B.; Białecki, T.; Łęgowik, A.; Merkisz, J.; Jasiński, R. Performance and Emissions of a Microturbine and Turbofan Powered by Alternative Fuels. *Aerospace* **2021**, *8*, 25. [CrossRef]
21. Kurzawska, P.; Jasiński, R. Overview of Sustainable Aviation Fuels with Emission Characteristic and Particles Emission of the Turbine Engine Fueled ATJ Blends with Different Percentages of ATJ Fuel. *Energies* **2021**, *14*, 1858. [CrossRef]
22. Merkisz, J.; Idzior, M.; Lijewski, P.; Fuc, P.; Karpiuk, W. The Analysis of the Quality of Fuel Spraying in Relation to Selected Rapeseed Oil Fuels for the Common Rail System. In Proceedings of the Ninth Asia-Pacific International Symposium on Combustion and Energy Utilization, Beijing, China, 2–6 November 2008; pp. 352–356.
23. Contreras, A.; Yigit, S.; Özay, K.; Veziroglu, T. Hydrogen as aviation fuel: A comparison with hydrocarbon fuels. *Int. J. Hydrog. Energy* **1997**, *22*, 1053–1060. [CrossRef]
24. Baroutaji, A.; Wilberforce, T.; Ramadan, M.; Olabi, A.G. Comprehensive investigation on hydrogen and fuel cell technology in the aviation and aerospace sectors. *Renew. Sustain. Energy Rev.* **2019**, *106*, 31–40. [CrossRef]
25. Christodoulakis, J.; Karinou, F.; Kelemen, M.; Kouremadas, G.; Fotaki, E.; Varotsos, C. Assessment of air pollution from Athens International Airport and suggestions for adaptation to new aviation emissions restrictions. *Atmos. Pollut. Res.* **2022**, *13*, 101441. [CrossRef]
26. Harrison, R.M.; Masiol, M.; Vardoulakis, S. Civil aviation, air pollution and human health. *Environ. Res. Lett.* **2015**, *10*, 041001. [CrossRef]
27. Owen, B.; Anet, J.G.; Bertier, N.; Christie, S.; Cremaschi, M.; Dellaert, S.; Edebeli, J.; Janicke, U.; Kuenen, J.; Lim, L.; et al. Review: Particulate Matter Emissions from Aircraft. *Atmosphere* **2022**, *13*, 1230. [CrossRef]
28. Spicer, C.W.; Holdren, M.W.; Cowen, K.A.; Joseph, D.W.; Satola, J.; Goodwin, B.; Mayfield, H.; Laskin, A.; Lizabeth Alexander, M.; Ortega, J.V.; et al. Rapid measurement of emissions from military aircraft turbine engines by downstream extractive sam-pling of aircraft on the ground: Results for C-130 and F-15 aircraft. *Atmos. Environ.* **2009**, *43*, 2612–2622. [CrossRef]
29. Chan, T.W.; Pham, V.; Chalmers, J.; Davison, C.; Chishty, W.; Poitras, P. Immediate impacts on particulate and gaseous emissions from a T56 turbo-prop engine using a biofuel blend. In *SAE Technical Paper Series, Proceedings of the SAE 2013 AeroTech Congress & Exhibition, Montreal, QC, USA, 24–26 September 2013*; SAE International 400 Commonwealth Drive: Warrendale, PA, USA, 2013.
30. Corporan, E.; Quick, A.; DeWitt, M.J. Characterization of Particulate Matter and Gaseous Emissions of a C-130H Aircraft. *J. Air Waste Manag. Assoc.* **2008**, *58*, 474–483. [CrossRef]
31. Cheng, M.-D.; Corporan, E.; DeWitt, M.J.; Spicer, C.W.; Holdren, M.W.; Cowen, K.A.; Laskin, A.; Harris, D.B.; Shores, R.C.; Kagann, R.; et al. Probing Emissions of Military Cargo Aircraft: Description of a Joint Field Measurement Strategic Environmental Research and Development Program. *J. Air Waste Manag. Assoc.* **2008**, *58*, 787–796. [CrossRef]
32. Jasiński, R.; Markowski, J.; Pielecha, J. Probe Positioning for the Exhaust Emissions Measurements. *Procedia Eng.* **2017**, *192*, 381–386. [CrossRef]
33. Ehyaei, M.A.; Anjiridezfuli, A.; Rosen, M.A. Fxergetic analysis of an aircraft turbojet engine with an afterburner. *Therm. Sci.* **2013**, *17*, 1181–1194. [CrossRef]
34. Misztal, A.; Szymanski, G.M.; Misztal, W.; Komorski, P. Innovative application of quality methods in the homogeneity assessment of the F-16 aircraft group in terms of generated noise. *Maint. Reliab.* **2022**, *24*, 187–199. [CrossRef]
35. Ardebili, S.M.S.; Kocakulak, T.; Aytav, E.; Calam, A. Investigation of the effect of JP-8 fuel and biodiesel fuel mixture on engine performance and emissions by experimental and statistical methods. *Energy* **2022**, *254*, 124155. [CrossRef]

36. Kinsey, J. *Personal Communication*; U.S. Environmental Protection Agency: Research Triangle Park, NC, USA, 2006.
37. Wey, C.C. Aircraft particle emissions eXperiment (APEX). In *Particulate Data Provided by National Aeronautics and Space Administration*; University of Missouri Rolla, Aerodyne Research Inc., and Wright Patterson Air Force Base: Cleveland, OH, USA, 2006.
38. Durdina, L.; Brem, B.; Abegglen, M.; Lobo, P.; Rindlisbacher, T.; Thomson, K.; Smallwood, G.; Hagen, D.; Sierau, B.; Wang, J. Determination of PM mass emissions from an aircraft turbine engine using particle effective density. *Atmos. Environ.* **2014**, *99*, 500–507. [CrossRef]
39. Timko, M.T.; Onasch, T.B.; Northway, M.J.; Jayne, J.T.; Canagaratna, M.R.; Herndon, S.C.; Wood, E.C.; Miake-Lye, R.C.; Knighton, W.B. Gas turbine engine emissions e Part II: Chemical properties of particulate matter. *ASME J. Eng. Gas Turbines Power* **2010**, *132*, 061505. [CrossRef]
40. Lobo, P.; Durdina, L.; Smallwood, G.J.; Rindlisbacher, T.; Siegerist, F.; Black, E.A.; Yu, Z.; Mensah, A.A.; Hagen, D.E.; Mi-ake-Lye, R.C.; et al. Measurement of aircraft engine non-volatile PM emissions: Results of the aviationparticle regulatory instrumentation demonstration exper-iment (A-PRIDE) 4 campaign. *Aerosol Sci. Technol.* **2015**, *49*, 472e484. [CrossRef]
41. Yu, Z.; Liscinsky, D.S.; Fortner, E.C.; Yacovitch, T.I.; Croteau, P.; Herndon, S.C.; Miake-Lye, R.C. Evaluation of PM emissions from two in-service gas turbine general aviation aircraft engines. *Atmos. Environ.* **2017**, *160*, 9–18. [CrossRef]
42. Lobo, P.; Hagen, D.E.; Whitefield, P.D. Measurement and analysis of aircraft engine PM emissions downwind of an active runway at the Oakland International Airport. *Atmos. Environ.* **2012**, *61*, 114–123. [CrossRef]
43. Kinsey, J.S.; Dong, Y.; Williams, D.C.; Logan, R. Physical characterization of the fine particle emissions from commercial aircraft engines during the Aircraft Particle Emissions eXperiment (APEX) 1–3. *Atmos. Environ.* **2010**, *44*, 2147–2156. [CrossRef]
44. Lopes, M.; Russo, A.; Monjardino, J.; Gouveia, C.; Ferreira, F. Monitoring of ultrafine particles in the surrounding urban area of a civilian airport. *Atmos. Pollut. Res.* **2019**, *10*, 1454–1463. [CrossRef]